Scattering and reactions of halo nuclei

Ronald C. Johnson

Department of Physics, School of Physics and Chemistry, University of Surrey, Guildford, Surrey, GU2 7XH, UK

Abstract. In these lectures I describe some of the key features of halo nuclei and how these features require a re-think of theories required to adequately describe their collisions with stable nuclei. I provide the basic scattering theory needed to understand few-body models of halo cross sections. The 'frozen halo' approximation is explained in detail and applications of the theory to elastic scattering, break-up and transfer reactions are discussed.

1 Introduction

Several times in the lectures at this Summer School we have been shown a picture of the N-Z plane with the valley of stability displayed and an indication of the position of the neutron and proton drip lines. There has been some emphasis on the properties of medium mass and heavy nuclei far from the valley of stability. My lectures will be mainly concerned with the neutron dripline in the region of small N and Z where very different types of phenomena occur and theories emphasise a different set of degrees of freedom than is usual in heavy nuclei.

One of the most exciting scientific developments in recent years has been the advent of accelerated beams of radioactive nuclei with exotic combinations of neutron and proton numbers. The new techniques produce beams of nuclei which decay by the weak interaction but are stable against decay into their constituents. Nuclear reactions induced by beams incident on targets of ordinary stable nuclei are important sources of information about the structure of the exotic species. For example, experiments of this type led to the discovery of the important new class of nuclei known as halo nuclei.[1–3]

New experiments are extending our understanding of these novel systems. The mechanisms involved in reactions involving haloes and other nuclei far from the valley of stability present a special challenge to theorists. An important consideration is that exotic nuclei are often very weakly bound and easily broken up in the Coulomb and nuclear fields of the target nucleus. Halo nuclei are an extreme case with almost zero binding energy. As a consequence, theories which address the special features associated with strong coupling to excited states of the projectile which may be in the continuum are a prerequisite if reliable information on nuclear structure is to be deduced from reaction experiments. On the other hand, many of the relevant experiments, both current and planned, involve projectile energies which allow simplifying assumptions to be made which help to make the theory more transparent. I will present some of the insights obtained in this way with illustrations from recent experiments.

J.M. Arias and M. Lozano (Eds.): LNP 581, pp. 259–291, 2001.

1.1 One-neutron halo nuclei

Key features of halo nuclei [4] remind us of some familiar features of the deuteron. For present purposes we can ignore the small deuteron D-state and consider the deuteron to be a $1S$ state in an attractive n-p potential of depth about 30MeV and range about 1 fm. The deuteron has a binding energy of $\varepsilon_d = 2.2$ MeV. Quantum mechanics tells us that in the classically forbidden region where the n-p separation r is bigger than 1fm the space part of the deuteron's wavefunction will have the form

$$\phi_0 = N_d \frac{\exp(-\lambda_d r)}{r}, \qquad r > 1\text{fm}, \tag{1}$$

where N_d is a normalisation constant. The constant λ_d is determined from the deuteron binding energy by $\lambda_d = \sqrt{2\mu\varepsilon_d/\hbar^2}$ where μ is the reduced mass of the n-p system. This is the functional form predicted by Yukawa for the interaction associated with the exchange of massive particles. Particle exchange also proceeds through classically forbidden regions and hence gives rise to the same functional dependence on distance.

The small deuteron binding energy results in the value $1/\lambda_d = 4.2$fm which is much larger than the range of the n-p interaction and means that in the deuteron the neutron and proton spend a significant part of the time in the classically forbidden region. Indeed, for many purposes its a good approximation to approximate the deuteron wavefunction by the form (1) for *all* values of r.

The one-neutron halo nucleus ^{11}Be can be described in a similar picture. It costs 0.503 MeV to remove a neutron from ^{11}Be and leave ^{10}Be in its ground state. The simplest version of the halo model describes the corresponding component of the ^{11}Be wavefunction as a ^{10}Be core and a neutron in an S-state. For n-core separations r bigger than the core radius the neutron wavefunction is

$$\phi_0 = N_{11} \frac{\exp(-\lambda_{11} r)}{r}, \tag{2}$$

where $1/\lambda_{11} = 6.7$ fm as detemined by the neutron separation energy.

The key point here is that $1/\lambda_{11}$ is much bigger than the size of the core so that the classically forbidden region outside the core plays a very important role, just as in the case of the deuteron.

There are however some important differences between the d and ^{11}Be cases. In the first place, unlike the deuteron, ^{11}Be has a bound excited state with a separation energy of 0.18 MeV. Secondly the Pauli principle demands that the ground state of ^{11}Be be a $2S$ state with a node in the core region in contrast with the nodeless function which simple potential models give for the deuteron. This reflects the fact that underlying this 2-body picture of ^{11}Be is a many fermion system.

The qualitative features associated with very weak binding suggests that an approach based on the 2-body picture might be a good starting point for studying the structure of ^{11}Be, in contrast with mean field models which emphasise the identity of all nucleons. It is this possibility of an alternative good starting point for models of their structure which makes halo systems interesting from

a theoretical point of view. For an excellent bibliography and a discussion of corrections to the basic few-body models see [5].

In these lectures I will concentrate on one-neutron halos. Much of what I have to say is also relevant to multi-neutron halos such as the famous two-neutron halo ^{11}Li [1,4].

2 Nuclear reaction theory

Nuclear reactions play a crucial role in the study of nuclei and halo nuclei are no exception. Well developed theories of nuclear reactions already exist [7]. The interesting questions for theory are whether these theories will work for reactions involving halo nuclei, and if not, how should they be modified.

The weak binding of halo nuclei makes a positive answer to the first question unlikely. The weak binding of the neutron to ^{11}Be, for example, means that the halo degree of freedom is easily excited by the nuclear and Coulomb fields of a target nucleus. The weak binding also means that even a small transfer of momentum from the relative motion of the 2 nuclei will excite the halo nucleus into the continuum of unbound states from which fragments may propagate to large distances. We have to learn how to treat such configurations realistically. This is especially difficult when the fragments are charged.

2.1 Few-body models

It is natural to base the reaction theory for halo systems on few-body models. Here I emphasise approaches which treat only the halo degrees of freedom explicitly, the other nuclear sub-systems being parameterised in terms of effective 2-body interactions.

As a concrete example we consider a 3-body model of reactions induced by a ^{11}Be projectile on a ^{12}C target. The 3 bodies involved are the ^{10}Be core and the halo neutron which make up our model of the projectile and the target. This system has been studied at GANIL at beam energies of 50 MeV/A.

A suitable set of co-ordinates to describe the system is shown in Figure 1. The Hamiltonian in the over-all centre of mass system is assumed to be

$$H = T_R + H_{nC} + V_{nT}(\boldsymbol{r}_{nT}) + V_{CT}(\boldsymbol{r}_{CT}), \tag{3}$$

where T_R is the total kinetic energy of the 3-bodies in the overall centre of mass system and H_{nC} is the Hamiltonian for the $n - C$ relative motion.

$$T_R = -\frac{\hbar^2}{2\mu_{PT}}\nabla_R^2, \quad H_{nC} = -\frac{\hbar^2}{2\mu_{nC}}\nabla_r^2 + V_{nC}(\boldsymbol{r}), \tag{4}$$

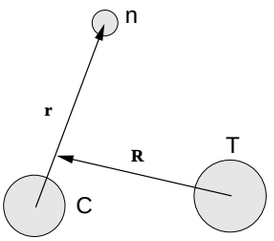

Fig. 1. Co-ordinates used in a 3-body model of a one neutron halo nucleus interacting with a target T

where μ_{PT} and μ_{nC} are reduced masses. The 2-body potentials V_{nC}, V_{CT} and V_{nT} are functions of the relative co-ordinates indicated as their arguments where

$$\boldsymbol{r}_{nT} = \boldsymbol{R} + \beta \boldsymbol{r}, \quad \beta = \frac{m_C}{m_P} \tag{5}$$

$$\boldsymbol{r}_{CT} = \boldsymbol{R} - \alpha \boldsymbol{r}, \quad \alpha = \frac{m_n}{m_P} \tag{6}$$

$$m_P = m_n + m_C. \tag{7}$$

These 2-body potentials depend only on relative co-ordinates and cannot excite the internal degrees of freedom of the core and the target nucleus. Such effects effects are taken into account implicitly by allowing V_{CT} and V_{nT} to be complex optical potentials which describe the relevant 2-body elastic scattering at the correct relative velocity. For weakly bound halo nuclei the latter can be taken to be the relative velocity of the projectile and target.

It is important to appreciate the significance of eigenfunctions of this model H. They are functions $\Psi(\boldsymbol{r}, \boldsymbol{R})$ which satisfy

$$H\Psi = E\Psi, \tag{8}$$

and describe that component of the true many-body wavefunction in which the target is in its ground state. The model eigenfunctions do have components in which the projectile is excited, but only those states which correspond to exciting the halo degrees of freedom including the continuum of break-up states. The model wavefunction can therefore only describe cross sections for elastic scattering, certain inelastic excitations of the projectile, elastic break-up of the projectile in which the target and core are left in their ground states, and the total reaction cross section.

2.2 Two-body scattering

In order to understand our approach to the 3-body system we must first remind ourselves of the formalism of 2-body scattering and learn how to express it in language which can be adapted to the many-body case.

The optical potential V_{nT} in the 3-body Hamiltonian (3) is a complex function of r_{nT} which is taken from the analysis of $n-T$ elastic scattering. It will usually have a Woods-Saxon shape, *i.e.*,

$$V_{nT}(r_{nT}) = \frac{-V_0 - iW_0}{1+\exp\left[(r_{nT}-R_0)/a\right]}, \tag{9}$$

where a typical value of the real depth parameter V_0 at low neutron energy is 40 MeV and the imaginary depth W_0 is about 0.26 V_0. The radius parameter R_0 is given by $1.2\mathrm{A}_T^{1/3}$ fm and the diffuseness $a = 0.65$ fm.

For V_{CT}, where C is ^{10}Be and T is ^{12}C, the analogous parameters would be $V_0 = 120$ MeV, $W_0 = 0.5V_0$, $R_0 = 0.75(\mathrm{A}_C^{1/3} + \mathrm{A}_T^{1/3})$ fm, $a = 0.65$ fm.

I emphasise that these values are quoted for illustration only. All the optical parameters may depend on the centre of mass energy of the interacting nuclei and may have a more sophisticated geometrical form than I have indicated above. For nuclei with spin there may be important spin dependent terms such as the familiar $\boldsymbol{L}.\boldsymbol{I}$ interaction and we should not forget that for charged particles there will be Coulomb terms which must be included. For 'ordinary' nuclei and the nucleon the systematics of the optical potential parameters are well understood. An important aspect of our approach is that we do not assume that these systematics apply to halo and other weakly bound nuclei. The few-body models allow us to input relatively well understood physics for the sub-systems which make up an exotic projectile.

To calculate the scattering of a particle from a target represented by a central potential $V(R)$ we have to solve the equation

$$(T_R + V(R))\chi(\boldsymbol{R}) = E\chi(\boldsymbol{R}), \tag{10}$$

where the kinetic energy operator T_R is as defined in (4) with an appropriate reduced mass. We require solutions which are regular at $R = 0$ and which for $R \to \infty$ in the direction $\hat{\boldsymbol{R}}$ satisfy

$$\chi(\boldsymbol{R}) \to \exp(i\boldsymbol{K}.\boldsymbol{R}) + f(\hat{\boldsymbol{R}})\exp(iKR)/R, \tag{11}$$

where $\boldsymbol{K}$ is the incident momentum. For present purposes I have ignored Coulomb forces (their long range introduces well understood technical complications in the 2-body problem), and spin dependence.

The elastic differential cross section is related to f by

$$\frac{d\sigma}{d\Omega_{\hat{\boldsymbol{R}}}} = \mid f(\hat{\boldsymbol{R}}) \mid^2 . \tag{12}$$

Calculating f for given V is a completely solvable problem. We use the fact that for a central V angular momentum is conserved just as in classical mechanics. This means that we can find solutions of (10) which are eigenfunctions of $\boldsymbol{L}^2$ and L_z where $\boldsymbol{L} = \boldsymbol{R} \wedge (i^{-1})\nabla_R$ is the angular momentum operator (in units of $\hbar$) and z is an arbitrary z-axis. Such solutions have the form

$$\chi(R,\theta,\phi) = \chi_{LM}(R)Y_{LM}(\theta,\phi), \tag{13}$$

where the angles (θ, ϕ) describe the direction of $\boldsymbol{R}$ in the chosen co-ordinate system. The spherical harmonics Y_{LM} are angular momentum eigenfunctions and satisfy

$$\boldsymbol{L}^2 Y_{LM} = L(L+1)Y_{LM}, \tag{14}$$

$$L_z Y_{LM} = M Y_{LM}. \tag{15}$$

The radial function $\chi_{LM}(R)$ satisfies the ordinary differential equation

$$-\frac{\hbar^2}{2\mu_{PT}}\frac{1}{R}\frac{d^2}{dR^2}(R\chi_{LM}(R)) + [V(R) + \frac{\hbar^2}{2\mu_{PT}}\frac{L(L+1)}{R^2}]\chi_{LM}(R) = E\chi_{LM}(R). \tag{16}$$

This equation has a unique solution within a constant of proportionality when the condition $\lim_{R\to 0} R\chi_{LM}(R) = 0$ is imposed.

For a finite range potential satisfying $V(R) = 0$, $R > R_0$ this unique solution has the form

$$\chi_{LM}(R) \stackrel{R>R_0}{=} \alpha(\cos\delta_L \, \mathrm{j}_L(KR) + \sin\delta_L \mathrm{n}_L(KR) \tag{17}$$

$$\stackrel{KR\gg L}{\to} \alpha \sin(KR - L\pi/2 + \delta_L)/KR, \tag{18}$$

where α is a constant independent of R and in the second line I have used the asymptotic forms of the regular and irregular spherical Bessel functions:

$$\mathrm{j}_L(KR) \stackrel{KR\gg L}{\to} \sin(KR - L\pi/2)/KR \tag{19}$$

$$\mathrm{n}_L(KR) \stackrel{KR\gg L}{\to} \cos(KR - L\pi/2)/KR. \tag{20}$$

In these equations the phase shifts δ_L appear. They are functions of energy and angular momentum and contain all the interesting dependence of the scattering on the potential V. The phaseshifts are complex if V is. The terminology is easily understood from eq.(18). If V is identically zero for all R the correct solution of eq.(16) is the spherical Bessel $\mathrm{j}_L(KR)$ with asymptotic form eqs.(19,20). Thus δ_L determines the phase difference at large distance between the free ($V = 0$) and the scattering wavefunction for a given L.

In order to relate the phase shifts to the scattering amplitude and hence to cross sections we must learn how to choose the c_{LM} so that the superposition

$$\chi(\boldsymbol{R}) = \sum_{LM} c_{LM}\chi_L^{(+)}(\boldsymbol{R})Y_{LM}(\hat{R}), \tag{21}$$

has the asymptotic form (11). I have added a (+) superscript to χ_L to designate that this function is normalized so that it satisfies eq. (17) with $\alpha = 1$.

It is easy to find the correct c_{LM}'s because we already know that the incident plane wave has the expansion

$$\exp i\boldsymbol{K}.\boldsymbol{R} = 4\pi \sum_{LM} i^L Y^*_{LM}(\hat{K})Y_{LM}(\hat{R})\mathrm{j}_L(KR). \tag{22}$$

A simple calculation using eqs.(18)-(22) and (11) gives

$$c_{LM} = 4\pi \exp(i\delta_L) i^L Y^*_{LM}(\boldsymbol{K}), \tag{23}$$

and hence

$$f^{(+)}(\theta,\phi) = 4\pi \sum_{LM} Y^*_{LM}(\hat{K}) Y_{LM}(\theta,\phi) \exp(i\delta_L) \sin\delta_L / K, \tag{24}$$

$$\chi^{(+)}_{\boldsymbol{K}}(\boldsymbol{R}) \quad = 4\pi \sum_{LM} i^L Y^*_{LM}(\hat{K}) Y_{LM}(\hat{R}) \exp(i\delta_L) \chi^{(+)}_L(R), \tag{25}$$

where (θ,ϕ) are the angles defining the direction of observation with respect to a chosen co-ordinate system.

Eq.(24) shows explicitly the relation between the scattering amplitude and the set of phase shifts. The scattering amplitude is related to the elastic differential cross section by eq.(12). The phase shifts also determine the total reaction cross section, which is a measure of the flux going into all channels except the elastic channel and is given by

$$\sigma_R = \frac{\pi}{K^2} \sum_L (2L+1)(1-|S_L|^2), \tag{26}$$

where

$$S_L = \exp(2i\delta_L), \tag{27}$$

is the elastic S-matrix (a 1x1 matrix in this special case).

Eq.(25) gives the relation between the full scattering state wavefunction in 3 dimensional space and its components with definite angular momentum L. The radial wavefunctions, $\chi^{(+)}_L(R)$, have an asymptotic form which is determined by the phase shifts. At finite distances $\chi^{(+)}_L(R)$ is determined obtained by solving the radial equation (16) numerically or otherwise. The phase-shift is found by matching the numerical value of the logarithmic derivative at some $R > R_0$ to the formula (17). Knowing the phase-shift the computed numerical values of the radial wavefunction can now be re-normalized so that it satisfies eq.(17) with $\alpha = 1$, thus defining $\chi^{(+)}_L(R)$.

The function $\chi^{(+)}_{\boldsymbol{K}}(\boldsymbol{R})$ defined in this way is an example of a 'distorted wave' . The subscript tells us that it is associated with an incident plane wave with momentum $\boldsymbol{K}$. This label does *not* mean that $\chi^{(+)}_{\boldsymbol{K}}(\boldsymbol{R})$ is an eigenfunction of the momentum operator with eigenvalue $\boldsymbol{K}$! The superscript (+) indicates that $\chi^{(+)}_{\boldsymbol{K}}(\boldsymbol{R})$ asymptotically has an *outgoing* spherical wave component. The complete asymptotic form is as in the RHS of eq.(11).

2.3 The mysterious $\chi^{(-)}_{\boldsymbol{K}}(\boldsymbol{R})$

In formulating theories of complex collisions we frequently come across other scattering states which asymptotically look like a plane wave plus an ingoing

spherical wave. We can construct such a state using the same radial wavefunctions by making a different choice for the c_{LM} in eq.(21) (simply change the factor $\exp i\delta_L$ in eq.(23) to $\exp -i\delta_L$.

In nuclear physics where the potentials V are frequently complex another case occurs. $\chi^{(-)}_{\boldsymbol{K}}(\boldsymbol{R})$ is defined to be a solution of eq.(10) with incoming spherical waves and with V replaced by its complex conjugate V^*:

$$(T_R + V^*(R))\chi^{(-)}_{\boldsymbol{K}}(\boldsymbol{R}) = E\chi^{(-)}_{\boldsymbol{K}}(\boldsymbol{R}). \tag{28}$$

It is easy to show that the radial part of this function must be the complex conjugate of $\chi^{(+)}_L$ within a multiplicative factor and hence does not require separate calculation and a new phase-shift. We find

$$\chi^{(-)}_{\boldsymbol{K}}(\boldsymbol{R}) \rightarrow \exp(i\boldsymbol{K}.\boldsymbol{R}) + f^{(-)}(\hat{\boldsymbol{R}})\exp(-iKR)/R, \tag{29}$$

$$f^{(-)}(\theta,\phi) = 4\pi\sum_{LM}(-1)^L Y^*_{LM}(\hat{K})Y_{LM}(\theta,\phi)\exp -i\delta^*_L \sin\delta^*_L/K, \tag{30}$$

$$\chi^{(-)}_{\boldsymbol{K}}(\boldsymbol{R}) = 4\pi\sum_{LM} i^L Y^*_{LM}(\hat{K})Y_{LM}(\hat{R})\exp -i\delta^*_L(\chi^{(+)}_L(R))^*. \tag{31}$$

With these definitions the precise relationship between $\chi^{(+)}$ and $\chi^{(-)}$ is

$$(\chi^{(-)}_{\boldsymbol{K}}(\boldsymbol{R}))^* = \chi^{(+)}_{-\boldsymbol{K}}(\boldsymbol{R}). \tag{32}$$

These 2 distorted waves and their multi-channel generalisations appear frequently in theories of nuclear reactions.

3 Formal methods

3.1 The 2-body case

We have seen that the problem of the scattering of 2 bodies interacting through a potential is completely solvable. We want to be able to recognise such solvable sub-problems when they appear in the formulation of many-body theories and to achieve this we must learn how to write the 2-body results in a more formal way.

We define the 2-body state $\mid \chi^{\varepsilon}_{\boldsymbol{K}} >$ as the solution of

$$(E + i\varepsilon - T_R - V) \mid \chi^{\varepsilon}_{\boldsymbol{K}} >= i\varepsilon \mid \boldsymbol{K} >, \tag{33}$$

where T_R is the kinetic energy operator and $\mid \boldsymbol{K} >$ is the incident plane wave state

$$< \boldsymbol{R} \mid \boldsymbol{K} >= \exp(i\boldsymbol{K}.\boldsymbol{R}) \tag{34}$$

Clearly for $\varepsilon \rightarrow 0$ the state $\mid \chi^{\varepsilon}_{\boldsymbol{K}} >$ satisfies the same equation as $\mid \chi^{(+)}_{\boldsymbol{K}} >$, eq.(10), but unlike the latter eq.(33) has the unique solution

$$\mid \chi^{\varepsilon}_{\boldsymbol{K}} >= \frac{i\varepsilon}{(E + i\varepsilon - T_R - V)} \mid \boldsymbol{K} >, \tag{35}$$

and incorporates the correct boundary conditions for $\varepsilon > 0$. To show this we re-write eq.(33) as

$$(E + i\varepsilon - T_R) \mid \chi^{\varepsilon}_{\boldsymbol{K}} >= i\varepsilon \mid \boldsymbol{K} > + V \mid \chi^{\varepsilon}_{\boldsymbol{K}} >, \tag{36}$$

and multiply both sides of this equation by the inverse of the operator $E + i\varepsilon - T_R$. We deduce

$$\begin{aligned} \mid \chi^{\varepsilon}_{\boldsymbol{K}} > &= \frac{i\varepsilon}{E + i\varepsilon - T_R} \mid \boldsymbol{K} > + \frac{1}{E + i\varepsilon - T_R} V \mid \chi^{\varepsilon}_{\boldsymbol{K}} > \\ &= \mid \boldsymbol{K} > + \frac{1}{E + i\varepsilon - T_R} V \mid \chi^{\varepsilon}_{\boldsymbol{K}} >, \end{aligned} \tag{37}$$

where we have used the result

$$(E - T_R) \mid \boldsymbol{K} >= 0. \tag{38}$$

When written out in configuration space eq.(37) is an integral equation for $\chi^{\varepsilon}_{\boldsymbol{K}}(\boldsymbol{R})$. In the same basis and for $\varepsilon \ll E$ and *positive* the matrix elements of $(E + i\varepsilon - T_R)^{-1}$ are

$$\begin{aligned} < \boldsymbol{R} \mid \frac{1}{E + i\varepsilon - T_R} \mid \boldsymbol{R}' > \quad &= \quad -\frac{2\mu}{4\pi\hbar^2} \frac{\exp{(iK|\boldsymbol{R} - \boldsymbol{R}'|)}}{|\boldsymbol{R} - \boldsymbol{R}'|} \exp{(-\frac{\varepsilon K|\boldsymbol{R} - \boldsymbol{R}'|}{2E})} \\ &\overset{R \gg R'}{\rightarrow} -\frac{2\mu}{4\pi\hbar^2} \frac{\exp{(iKR - i\boldsymbol{K}'.\boldsymbol{R}')}}{R} \exp{(-\frac{\varepsilon KR}{2E})}, \end{aligned} \tag{39}$$

where $\boldsymbol{K}'$ has the same magnitude as $\boldsymbol{K}$ but points in the direction (θ, ϕ) of $\boldsymbol{R}$. The quantity μ is the reduced mass of the 2-body system.

Using (39) in (37) we find that for R well outside the range of V but not large compared with $\frac{2E}{\varepsilon K}$

$$\chi^{\varepsilon}_{\boldsymbol{K}}(\boldsymbol{R}) \rightarrow \exp{(i\boldsymbol{K}.\boldsymbol{R})} + f^{\varepsilon}(\theta, \phi) \frac{\exp{(iK - \frac{\varepsilon K}{2E})R}}{R}, \tag{40}$$

where

$$f^{\varepsilon}(\theta, \phi) = -\frac{2\mu}{4\pi\hbar^2} < \boldsymbol{K}' \mid V \mid \chi^{\varepsilon}_{\boldsymbol{K}} > . \tag{41}$$

The scattering amplitude f introduced in (11) is given by

$$\begin{aligned} f &= \lim_{\varepsilon \rightarrow 0^+} f^{\varepsilon}, \\ &= -\frac{2\mu}{4\pi\hbar^2} < \boldsymbol{K}' \mid V \mid \chi^{(+)}_{\boldsymbol{K}} > . \end{aligned} \tag{42}$$

The amplitude f^{ε} also has a physical meaning. It can be thought of as the scattering amplitude for an incident wave packet with a spread in time of order $\hbar/\varepsilon$[8].

Eq.(42) expresses the scattering amplitude as a matrix element of the potential V between a plane wave describing the final observed state and the distorted

wave $\mid \chi^{(+)}_{\boldsymbol{K}} >$ which, of course, also depends implicitly on V. This expression does not at first sight appear very useful as a way of determining V. However this type of expression, especially when generalised to systems with many degrees of freedom, lends itself well to generating useful insights and approximations.

As a simple application, let us suppose that the potential V is very weak. Then one would expect that to first order in V the distorted wave in (42) might usefully approximated by the incident plane wave $\mid \boldsymbol{K} >$. The resulting formula is the famous Born approximation

$$\begin{aligned} f^{Born} &= -\frac{2\mu}{4\pi\hbar^2} < \boldsymbol{K'} \mid V \mid \boldsymbol{K} > \\ &= -\frac{2\mu}{4\pi\hbar^2} \int d\boldsymbol{R} \exp{(i\boldsymbol{Q}\cdot\boldsymbol{R})} V(R), \end{aligned} \tag{43}$$

where $\boldsymbol{Q}$ is the momentum transfer, $\boldsymbol{Q} = \boldsymbol{K} - \boldsymbol{K'}$.

Another way of looking at the matrix element in (42) it to relate it to a matrix element of a new operator $\mathcal{T}(E + i\varepsilon)$ defined by

$$\mathcal{T}(E + i\varepsilon) = V + V \frac{1}{E + i\varepsilon - T_R - V} V. \tag{44}$$

Acting on a plane wave with momentum $\boldsymbol{K}$ related to E by

$$K = \sqrt{\frac{2\mu E}{\hbar^2}}, \tag{45}$$

we find

$$\begin{aligned} \mathcal{T}(E + i\varepsilon) \mid \boldsymbol{K} > &= V \frac{1}{E + i\varepsilon - T_R - V} [(E + i\varepsilon - T_R - V) + V] \mid \boldsymbol{K} > \\ &= V \frac{i\varepsilon}{E + i\varepsilon - T_R - V} \mid \boldsymbol{K} > \\ &= V \mid \chi^{(+)}_{\boldsymbol{K}} >, \end{aligned} \tag{46}$$

where we have used the result (35) to identify $\mid \chi^{(+)}_{\boldsymbol{K}} >$ in the 2nd line in (46). Taking the inner product of both sides of (46) with a plane wave state $\mid \boldsymbol{K'} >$, where $\boldsymbol{K'}$ has the same magnitude as $\boldsymbol{K}$ and is given by (45), we obtain

$$f^{\varepsilon}(\theta, \phi) = -\frac{2\mu}{4\pi\hbar^2} < \boldsymbol{K'} \mid \mathcal{T}(E + i\varepsilon) \mid \boldsymbol{K} > . \tag{47}$$

The operator $\mathcal{T}(E + \varepsilon)$ has matrix elements between plane wave states with arbitrary momentum. It is only when the initial and final momenta are related to E by [45] that these so-called on-shell matrix elements are related to the scattering amplitude. The half-on-shell matrix elements with $K$and E related by [45] but K' arbitrary determine the distorted wave $\mid \chi^{(+)}_{\boldsymbol{K}} >$. To see this we use the last line in (37) and the result (46) to obtain

$$\begin{aligned} \mid \chi^{\varepsilon}_{\boldsymbol{K}} > &= \mid \boldsymbol{K} > + \frac{1}{E + i\varepsilon - T_R} \mathcal{T}(E + i\varepsilon) \mid \boldsymbol{K} > \\ &= \mid \boldsymbol{K} > + \int d\boldsymbol{K'} \frac{\mid \boldsymbol{K'} >< \boldsymbol{K'} \mid \mathcal{T}(E + i\varepsilon) \mid \boldsymbol{K} >}{E + i\varepsilon - E'}, \end{aligned} \tag{48}$$

where

$$E' = \frac{\hbar^2 (K')^2}{2\mu}. \tag{49}$$

We see that all quantities of physical interest are determined by the $\mathcal{T}$-operator. Conversely, both the on-shell and half-off-shell matrix elements of $\mathcal{T}$ can be found by solving the Schrödinger equation for $\mid \chi^+_{\boldsymbol{K}} >$.

An important advantage of the formal methods we have introduced in this section is that they allow us to manipulate explicit expressions for wavefunctions and scattering amplitudes using the rules of operator algebra without having to deal with singular operators. For $\varepsilon \neq 0$ operators like $(E + i\varepsilon - H)^{-1}$ exist for any real E and for Hamiltonians H of physical interest. Boundary conditions have been taken care of once and for all by the ε prescription. The price we have to pay is that in carrying out these manipulations we have to remember thet the scattering states satisfy inhomogeneous equations such as eq.(33) rather than eigenvalue equations like eq.(10).

Of course at the end of the day we are interested in the limit $\varepsilon \to 0^+$. In the many-body case this limit has to be taken with care, but in practical nuclear reaction calculations this does not usually cause a problem. Difficulties with this limiting process can arise, for example, in the formulation of exact numerical solutions of the 3-body scattering problem. A re-formulation in terms of the Faddeev equations is then an advantage, but for the purpose of exposing the structure of many body theories this step and its generalisations to more than 3 bodies is not necessary.

3.2 Target with internal degrees of freedom

For definiteness we consider the scattering of a neutron from a target A which has a set of bound states $\phi_0(\xi), \phi_2(\xi), \ldots, \phi_N(\xi)$ where ξ denotes the set of internal co-ordinates of A. By convention 0 labels the ground state, 1 the first excited state, and so on. The generalisation of the eq.(10) is

$$(T_R + H_A + V(\boldsymbol{R}, \xi))\chi(\boldsymbol{R}, \xi) = E\chi(\boldsymbol{R}, \xi), \tag{50}$$

where H_A is the Hamiltonian which describes the internal motion of A. T_R is the total kinetic energy operator of the neutron and the target in the overall centre of mass system and is defined in eq.(4) with a reduced mass μ_{nT}. $\boldsymbol{R}$ is the relative co-ordinate of the neutron and the centre of mass of A. The potential term $V(\boldsymbol{R}, \xi)$ depends on both $\boldsymbol{R}$ and ξ. It describes the interaction between the neutron and the target and at the most basic level can be expressed as the sum of the 2-body interactions between the neutron and the target nucleons. The ξ would then denote the co-ordinates of the target nucleons relative to its centre of mass.

One approach to solving eq.(50) is to expand χ as a superposition of the set of states ϕ_i which form a complete set if all possible states of A are included. The coefficients in the expansion are functions of $\boldsymbol{R}$ which are the solution of a set of coupled differential equations.

The expansion is

$$\chi(\boldsymbol{R},\xi) = \chi_0(\boldsymbol{R})\phi_0(\xi) + \chi_1(\boldsymbol{R})\phi_1(\xi) + \ldots \tag{51}$$

Coupled equations are obtained by substituting the expansion (51) into (50), multiplying by ϕ_i and integrating over all ξ for $i = 0,\ 1\ldots, N$. The resulting equations for $i = 0,\ 1\ldots, N$ are

$$(E_i - T_R - V_{ii})\chi_i = \sum_{j\neq i} V_{ij}\chi_j, \tag{52}$$

where we have used the eigenvalue equations satisfied by the ϕ_i and their orthonormality relations

$$H_A\phi_i = \epsilon_i\phi_i, \tag{53}$$

$$\int d\xi \phi_i^*\phi_j\ = \delta_{ij}. \tag{54}$$

The energies E_i are defined by $E_i = E - \epsilon_i$.

The coupling potentials V_{ij} are functions of $\boldsymbol{R}$ defined by

$$V_{ij}(\boldsymbol{R}) = \int d\xi \phi_i^*(\xi)V(\boldsymbol{R},\xi)\phi_j(\xi). \tag{55}$$

The functions $\chi_i(\boldsymbol{R})$ have a definite physical meaning. They tell us the relative probability as a function of $\boldsymbol{R}$ for the target A being in state i. The different possibilities for i are frequently referred to as 'channels' and the E_i are the corresponding channel energies. If the incident channel is $i = 0$ the boundary conditions to be satisfied by the χ_i for values of R outside the range of the coupling potentials are

$$\chi_0^{(+)} \to \exp(i\boldsymbol{K}_0.\boldsymbol{R}) + f_{00}^{(+)}(\hat{\boldsymbol{R}})\exp(iK_0R)/R, \tag{56}$$

$$\chi_i^{(+)} \to f_{i0}(\hat{\boldsymbol{R}})\exp(iK_iR)/R, \quad i \neq 0 \tag{57}$$

where the channel momenta K_i are defined by

$$K_i = \sqrt{\frac{2\mu_{nT}E_i}{\hbar^2}}, \tag{58}$$

provided that $E_i > 0$. If $E_i < 0$ the channel is said to be 'closed' and the corresponding χ_i vanishes exponentially at large distances. There is therefore no outgoing flux in a closed channel and the crosssection for exciting the target into state i will vanish.

If the potentials $V_{ij} = 0$ vanish for $i \neq j$ there will be no coupling between channels. In this limit the regular solution of the coupled equations satisfying the conditions (57) is $\chi_i = 0$ for $i \neq 0$ and χ_0 satisfies

$$(E_0 - T_R - V_{00})\chi_0 = 0. \tag{59}$$

Only the cross section for the elastic scattering of the neutron by the target in its ground state is non zero.

According to (59) elastic scattering in the zero coupling case is generated by V_{00} which has the explicit expression (we assume the ground state has spin 0 for simplicity)

$$\begin{aligned} V_{00}(\boldsymbol{R}) &= \int d\xi \phi_0^*(\xi) V(\boldsymbol{R}, \xi) \phi_o(\xi). \\ &= \sum_i \int d\xi \mid \phi_0(\xi) \mid^2 v_{ni}(\boldsymbol{R} - \boldsymbol{r}_i) \end{aligned} \tag{60}$$

where the summation over i includes all the nucleons in the target and the $\boldsymbol{r}_i$ are the co-ordinates of the target nucleons relative to the target centre of mass. If the target consists of A identical nucleons (60) reduces to

$$V_{00}(\boldsymbol{R}) = A \int d\boldsymbol{r}_1 \rho(\boldsymbol{r}_1) v_{n1}(\boldsymbol{R} - \boldsymbol{r}_1), \tag{61}$$

where $\rho(\boldsymbol{r}_1)$ is the ground state one-body density of the target.

Eq.(61) is the simplest possible model for the optical potential. It relates the effective interaction between the projectile and the target to the fundamental 2-body interactions between the projectile and the target constituents and their density distribution in space. Eq(61) is often referred to as the folding model because of the way the co-ordinates appear in the integral in (61). Note that if the 2-body interaction v_{ni} is real so is V_{00}. This model cannot account for the imaginary part of the optical potential because it corresponds to a theoretical model where no flux is lost to non-elastic channels. We will see below by explicit calculation in a special case how open inelastic channels give rise to a complex effective interaction.

3.3 Formal theory of the multi-channel case

The formal approach developed in Subsection 3.1 is easily generalised to include the possibility that the target has internal degrees of freedom. Eq.(33) is replaced by

$$(E + i\varepsilon - T_R - H_A - V) \mid \chi^{\varepsilon}_{\boldsymbol{K}_0} >= i\varepsilon \mid \boldsymbol{K}_0, \phi_0 >, \tag{62}$$

where

$$< \boldsymbol{R}, \xi \mid \boldsymbol{K_0}, \phi_0 >= \exp(i\boldsymbol{K}_0.\boldsymbol{R}) \phi_0(\xi). \tag{63}$$

is the wavefunction corresponding to a plane wave incident on the target in its ground state.

The presence of the $i\varepsilon$ term on the right hand side of (62) means that the coupled equations equivalent to (52) are

$$(E_i + i\varepsilon - T_R - V_{ii}) \mid \chi_i^{\varepsilon} > = \sum_{j \neq i} V_{ij} \mid \chi_j^{\varepsilon} > + \delta_{i0} \mid \boldsymbol{K}_0 >, \tag{64}$$

where the channel components are related to $\mid \chi^{\varepsilon}_{\boldsymbol{K}_0} >$ by

$$\chi^{\varepsilon}_{\boldsymbol{K}_0}(\boldsymbol{R},\xi) = \sum_i \chi^{\varepsilon}_i(\boldsymbol{R})\phi_i(\xi). \tag{65}$$

For $N = 1$ (2 channels) these equations reduce to

$$(E_0 + i\varepsilon - T_R - V_{00}) \mid \chi^{\varepsilon}_0 > = V_{01} \mid \chi^{\varepsilon}_1 > + \mid \boldsymbol{K}_0 >, \tag{66}$$

$$(E_1 + i\varepsilon - T_R - V_{11}) \mid \chi^{\varepsilon}_1 > = V_{10} \mid \chi^{\varepsilon}_0 > . \tag{67}$$

The second equation allows us to express $\mid \chi^{\varepsilon}_1 >$ in terms of $\mid \chi^{\varepsilon}_0 >$ as

$$\mid \chi^{\varepsilon}_1 >= (E_1 + i\varepsilon - T_R - V_{11})^{-1} V_{10} \mid \chi^{\varepsilon}_0 > . \tag{68}$$

Substituting this result into the first of eqs.(67) gives an equation for $\mid \chi^{\varepsilon}_0 >$ which is

$$(E_0 + i\varepsilon - T_R - V_{00} - V_{01}(E_1 + i\varepsilon - T_R - V_{11})^{-1} V_{10} \mid \chi^{\varepsilon}_0 >=\mid \boldsymbol{K}_0 > . \tag{69}$$

We recognise this as a 2-body elastic scattering equation for $\mid \chi^{\varepsilon}_0 >$ with the effective potential

$$\mathcal{V}_{opt} = V_{00} + V_{01}(E_1 + i\varepsilon - T_R - V_{11})^{-1} V_{10} \tag{70}$$

This analysis shows how an effective potential can always be found which generates the exact elastic scattering. Note that the second term in eq.(70) has an imaginary part in the limit $\varepsilon \to 0^+$, but only if $E_1 > 0$, *i.e.*. above the threshold for exciting the state ϕ_1. Furthermore this imaginary part is negative, indicating that it is associated with a loss of probability flux from the incident channel. Our treatment of the $N = 1$ problem is a special case of a general theory due to Feshbach[6]. A discussion of effective interactions including the effect of energy averaging and additional references can be found in Section 2.9 of ref.[7].

3.4 Inelastic scattering and the DWBA

From eq.(68) we obtain an explicit expression for the amplitude for exciting the state ϕ_1. We use the operator identity

$$\frac{1}{A} - \frac{1}{B} = \frac{1}{A}(B - A)\frac{1}{B}, \tag{71}$$

to deduce

$$\frac{1}{(E_1 + i\varepsilon - T_R - V_{11})} = \frac{1}{(E_1 + i\varepsilon - T_R)}\left[1 + V_{11}\frac{1}{(E_1 + i\varepsilon - T_R - V_{11})}\right], \tag{72}$$

and therefore

$$\mid \chi^{\varepsilon}_1 >= \frac{1}{(E_1 + i\varepsilon - T_R)}\Omega_1^{(-\varepsilon)\dagger} V_{10} \mid \chi^{\varepsilon}_0 >, \tag{73}$$

where

$$\Omega_1^{(-\varepsilon)} = \left[1 + \frac{1}{(E_1 - i\varepsilon - T_R - V_{11})} V_{11}\right]. \tag{74}$$

Following similar reasoning as in the analysis surrounding eq.(40) we find that for $R \to \infty$ and $\varepsilon \to 0^+$

$$< \boldsymbol{R} \mid \chi_1^+ > \to f_{10}^{(+)} \frac{\exp{(iK_1 R)}}{R}, \tag{75}$$

where

$$f_{10}^{(+)} = -\frac{2\mu}{4\pi\hbar^2} < \boldsymbol{K}_1 \mid \Omega_1^{(-)\dagger} V_{10} \mid \chi_0^{(+)} >, \tag{76}$$

and the wave number $\boldsymbol{K}_1$ is in the direction of observation and has magnitude

$$K_1 = \sqrt{\frac{2\mu}{\hbar^2} E_1}. \tag{77}$$

Note that in eq.(76), $\chi_0^{(+)}$ is the exact elastic scattering distorted wave as generated by $\mathcal{V}_{opt}$, or by solving the coupled equations (67).

It can be shown that for $\varepsilon \to 0$ through positive values

$$< \boldsymbol{K}_1 \mid \Omega_1^{(-)\dagger} =< \chi_{\boldsymbol{K}_1}^{(-)} \mid, \tag{78}$$

where $\mid \chi_{\boldsymbol{K}_1}^{(-)} >$ is a distorted wave of the type defined in Sub-section 2.3 and generated by the potential V_{11}. The inelastic scattering amplitude (76) can therefore be written

$$f_{10}^{(+)} = -\frac{2\mu}{4\pi\hbar^2} < \chi_{\boldsymbol{K}_1}^{(-)} \mid V_{10} \mid \chi_{\boldsymbol{K}_0}^{(+)} >, \tag{79}$$

where we have written χ_0^{ε} as $\chi_{\boldsymbol{K}_0}^{(+)}$ to conform to our earlier notation in the limit $\varepsilon \to 0$.

The DWBA as originally formulated can be obtained from this exact expression by replacing the initial distorted wave by the distorted wave generated by the potential V_{00} instead of $\mathcal{V}_{opt}$. This approximation includes the diagonal elements V_{11} and V_{00} to all orders but the potential V_{10} responsible for coupling the 2 channels is included in first order only. The usual Born approximation of inelastic scattering corresponds to replacing the 2 distorted waves by plane waves. The DWBA attempts to do better than that by recognising that the target-projectile interaction will scatter the 2 nuclei and convert the plane waves into distorted plane waves. The DWBA is a consistent way to take this physical effect into account when the channel coupling is weak enough to be treated to 1st order.

We emphasise that in the realistic multi-channel situation we frequently meet in nuclear physics the DWBA as just defined is rarely used. An expression with a structure similar to (79) is used but with the 2 distorted waves generated by complex potentials which fit elastic scattering data. This is called the 'Distorted Wave Method' by Satchler [7]. Modern computer methods emphasise exact solutions of coupled channels models although Distorted Wave ideas often still underlie much qualitative thinking about nuclear reactions.

3.5 Practical evaluation of DW matrix elements

It is useful to have some insight into how expressions such as (79) are actually evaluated. For central distorting potentials the 2 distorted waves have expansions of the form introduced in subsection 2.2. We can write

$$\chi^{(+)}_{\boldsymbol{K}_0}(\boldsymbol{R}) \quad = 4\pi \sum_{L_0 M_0} i^{L_0} Y^*_{L_0 M_0}(\hat{K_0}) Y_{L_0 M_0}(\Omega_R) \exp{(i\delta^0_{L_0})} \chi^{(+)}_{L_0}(R), \tag{80}$$

$$(\chi^{(-)}_{\boldsymbol{K}_1}(\boldsymbol{R}))^* = 4\pi \sum_{L_1 M_1} (-1)^{L_1} i^{L_1} Y_{L_1 M_1}(\hat{K_1}) Y^*_{L_1 M_1}(\Omega_R) \exp{(i\delta^1_{L_1})} \chi^{(+)}_{L_1}(R) \tag{81}$$

Inserting these expressions into (79) we obtain

$$f^{(+)}_{10} = -\frac{8\pi\mu}{\hbar^2} \sum_{L_0 M_0 L_1 M_1} i^{L_0 - L_1} Y^*_{L_0 M_0}(\hat{K_0}) Y_{L_1 M_1}(\hat{K_1}) \exp{i(\delta^0_{L_0} + \delta^1_{L_1})} \tag{82}$$

$$\times \int_0^\infty R^2 dR \chi^{(+)}_{L_1}(R) < L_1 M_1 \mid V_{10} \mid L_0 M_0 > \chi^{(+)}_{L_0}(R), \tag{83}$$

with summation over L_0, M_0, L_1, M_1. Integration over the direction of $\boldsymbol{R}$ and the internal co-ordinates of the target are contained in the matrix element $< L_1 M_1 \mid V_{10} \mid L_0 M_0 >$

$$< L_1 M_1 \mid V_{10} \mid L_0 M_0 >= \int d\Omega_R \, d\xi \, Y^*_{L_1 M_1}(\Omega_R) \phi^*_1(\xi) V_{10}(\boldsymbol{R}, \xi) \phi_0(\xi) Y_{L_0 M_0}(\Omega_R). \tag{84}$$

By making a multipole expansion of the interaction V_{10} this matrix element can be factorised into reduced multipole matrix elements, which contain all the dependence on the structure of the target states ϕ_0 and ϕ_1, Clebsch-Gordan coefficients which carry the implications of angular momentum conservation and form factors which depend on the radial co-ordinate R (see,*e.g.*, Section 5.6 of ref.[7]). We do not have space to expand further on these important ideas here.

Standard codes exist which evaluate DW amplitudes such as (83) and solve the coupled equations (52) exactly for given poentials and target wave functions as a routine matter [12].

We note that most of the formulae in this section have to be modified when the nuclei involved are charged. The formal expressions we have used are perfectly valid when all the Coulomb interactions are screened at large distances. The correct expressions to be used for partial wave expansions when the uninteresting dependence on the screening radius is extracted are given in many standard texts, *eg*, [7]. Recent reviews which include Coulomb and spin-dependent effects can be found in [13] and [14].

3.6 Many-body $\mathcal{T}$-operator

As in the 2-body case we introduce an operator $\mathcal{T}$ whose on-shell matrix elements are proportional to the inelastic and inelastic scattering amplitudes. The key

difference is that this operator now acts in the space of the variables ξ as well as $\boldsymbol{R}$. The definition of $\mathcal{T}$ is

$$\mathcal{T}(E+i\varepsilon) = V + V\frac{1}{E+i\varepsilon - T_R - H_A - V}V. \tag{85}$$

This expression has exactly the same formal structure as (44) in the 2-body case, but the presence of the target Hamiltonian, H_A in the denominator in (85) makes this $\mathcal{T}$ a much more complicated operator.

In terms of $\mathcal{T}$ the elastic and inelastic scattering amplitudes are given by

$$f^{\varepsilon}(\theta,\phi)_{i0} = -\frac{2\mu}{4\pi\hbar^2} < \boldsymbol{K}_i, \phi_i \mid \mathcal{T}(E+i\varepsilon) \mid \boldsymbol{K}_0, \phi_0 >, \tag{86}$$

and the scattering state is expreessed in terms of the off-shell matrix elements of $\mathcal{T}$ through

$$\mid \chi^{\varepsilon}_{\boldsymbol{K}_0} >= \mid \boldsymbol{K}_0, \phi_0 > + \sum_i \int d\boldsymbol{K}' \frac{\mid \boldsymbol{K}', \phi_i >< \boldsymbol{K}', \phi_i \mid \mathcal{T}(E+i\varepsilon) \mid \boldsymbol{K}_0, \phi_0 >}{E_0 + \epsilon_0 + i\varepsilon - E' - \epsilon_i}. \tag{87}$$

The point about these formal expressions is that they help us to recognise quantities that are calculable using standard techniques when they are buried in a complicated theory of a nuclear reaction. To calculate a matrix element of a $\mathcal{T}$ operator in practice one usually, but not always re-expresses the calculation in terms of coupled differential equations.

4 Scattering of halo nuclei

We now return to the consideration of few-body models of the scattering of halo systems introduced in Section 2.1. As in that Section I will take as a specific example a 3-body model of reactions induced by a ^{11}Be projectile on a ^{12}C target. The 3 bodies involved are the ^{10}Be core and the halo neutron, which make up our model of the projectile, and the target.

The Hamiltonian in the over-all centre of mass system is that given in eq.(3) which I repeat here for convenience.

$$H = T_R + H_{nC} + V_{nT}(\boldsymbol{r}_{nT}) + V_{CT}(\boldsymbol{r}_{CT}). \tag{88}$$

Possible states of the halo are eigenstates of H_{nC} and satisfy

$$\begin{aligned} (H_{nC} - \epsilon_i)\phi_i(\boldsymbol{r}) &= 0, \ i = 0, 1, 2 \ldots, \\ (H_{nC} - \epsilon_k)\phi_{\boldsymbol{k}}(\boldsymbol{r}) &= 0, \quad \epsilon_k = \frac{\hbar^2 k^2}{2\mu_{nC}}, \end{aligned} \tag{89}$$

where we have distinguished between discrete bound states labelled by i and the continuum states labelled by momentum $\boldsymbol{k}$. Transitions to the latter correspond to elastic break-up.

One approach to finding scattering state solutions to eq.(8) is to proceed as in Section 3.2 and look for solutions as an expansion in the complete of functions of $\boldsymbol{r}$ defined in eq.(89):

$$\Psi(\boldsymbol{R},\boldsymbol{r}) = \phi_0(\boldsymbol{r})\chi_0(\boldsymbol{R}) + \phi_1(\boldsymbol{r})\chi_1(\boldsymbol{R}) + \cdots , \\ + \int d\boldsymbol{k}\phi_{\boldsymbol{k}}(\boldsymbol{r})\chi_{\boldsymbol{k}}(\boldsymbol{R}). \tag{90}$$

The functions $\chi_i(\boldsymbol{R}),\ \chi_{\boldsymbol{k}}(\boldsymbol{R})$ in eq.(90) give the amplitudes for exciting the various halo states. All of them have the form of outgoing spherical waves at large R with amplitudes which determine the corresponding excitation cross sections. The function $\chi_0(\boldsymbol{R})$ also includes a plane wave describing the incident beam.

The χ's satisfy a set of coupled differential equations which, if we ignore the continuum terms in eq.(90), have the form

$$(E_0 - T_{\boldsymbol{R}} - V_{ii}(\boldsymbol{R}))\chi_i(\boldsymbol{R}) = \sum_{j\neq i} V_{ij}(\boldsymbol{R})\chi_j(\boldsymbol{R}) \\ i,\ j = 0,\ 1, \ldots , \tag{91}$$

where $E_i = E - \epsilon_i$ and the coupling potentials $V_{ij}(\boldsymbol{R})$ are given by

$$V_{ij} = \int d\boldsymbol{r}\phi_i^*(\boldsymbol{r})[V_{nT}(\boldsymbol{R}+\beta\boldsymbol{r}) + V_{CT}(\boldsymbol{R}-\alpha\boldsymbol{r})]\phi_j(\boldsymbol{r}). \tag{92}$$

The coupling potentials describe the way tidal forces generated by the interactions between the components C and n of the projectile and the target can cause excitations of the projectile. It is the variation of the potentials on a scale of the order of the size of the projectile which generate terms with $i \neq j$ which would otherwise vanish by the orthogonality of the $\phi_j(\boldsymbol{r})$.

When the continuum terms on the right hand side of eq.(90) are included the generalisation of eq.(91) now includes coupling terms which couple discrete and continuum terms as well as terms coupling the continuum to itself. These terms involve coupling potentials like eq.(92) but with at least one of the $\phi_i(\boldsymbol{r})$ replaced by a $\phi_{\boldsymbol{k}}(\boldsymbol{r})$. These are the couplings which induce break-up of the halo and which are expected to play a prominent role in reactions involving halo nuclei.

One way of handling these equations when continuum couplings are important is to map the continuum onto a discrete square-integrable basis which is orthogonal to the bound states ϕ_i. This CDCC method pioneered by the Kyushu Group [15,16] makes use of this idea. This approach has been successfully applied to the scattering of deuterons and other loosely bound nuclei but has difficulties when long range Coulomb couplings are included [17]. This approach will not be considered in detail here. Instead we will discuss a widely used approximation to the many-body scattering problem which is sometimes much simpler to implement than the CDCC method and provides interesting insights into the role of the continuum in the scattering of halo nuclei.

4.1 Adiabatic approximation

The adiabatic approximation is based on the observation that at sufficiently high incident energy the halo degrees of freedom may be regarded as 'frozen' over the time needed for the projectile to traverse the target. This does *not* mean that we assume that the projectile remains in the same eigenstate ϕ_0 of H_{nC}, but rather that the co-ordinate $\boldsymbol{r}$ is frozen. This approximation is at the basis of Glauber's theory of composite particle scattering [18], versions of which have been widely used in the analysis of reactions involving halo nuclei. The adiabatic approximation retains its usefulness, however, even when the other assumption of Glauber's theory, *i.e.*, the eikonal approximation, is not invoked.

We can get some insight into the validity of the adiabatic approximation and how it can be implemented by considering the time dependent version of eq.(8)

$$H\Psi(\boldsymbol{R},\ \boldsymbol{r},\ t) = i\hbar\partial\Psi(\boldsymbol{R},\ \boldsymbol{r},\ t)/\partial t. \tag{93}$$

The substitution

$$\Psi = \exp(-i(H_{nC} - \epsilon_0)t/\hbar)\Phi, \tag{94}$$

transforms eq.(93) into the equivalent form

$$(T_R + \epsilon_0 + V_{nT}(\boldsymbol{R} + \beta\boldsymbol{r}(t)) + V_{CT}(\boldsymbol{R} - \beta\boldsymbol{r}(t)))\Phi = i\hbar\partial\Phi/\partial t, \tag{95}$$

where the term in H_{nC} has been removed at the expense of a time dependent $\boldsymbol{r}(t)$ satisfying

$$\boldsymbol{r}(t) = \exp(i(H_{nC} - \epsilon_0)t/\hbar)\ r\ \exp(-i(H_{nC} - \epsilon_0)t/\hbar). \tag{96}$$

The adiabatic approximation replaces $\boldsymbol{r}(t)$ by $\boldsymbol{r}(0) = \boldsymbol{r}$ in eq.(95). A sufficient condition for this to be accurate over the collision time t_{coll} is

$$(H_{nC} - \epsilon_0)t_{coll}/\hbar \ll 1. \tag{97}$$

When this adiabatic condition is satisfied, stationary state solutions of eq.(95) satisfy

$$(T_R + V_{nT}(\boldsymbol{R} + \beta\boldsymbol{r}) + V_{CT}(\boldsymbol{R} - \beta\boldsymbol{r}))\Phi = E_K\Phi, \tag{98}$$

where $E_K = E - \epsilon_0$ is the incident kinetic energy and we have assumed a time dependent factor $\exp(-iEt/\hbar)$ for times satisfying eq.(97).

In eq.(98) $\boldsymbol{r}$ is no longer a dynamical variable but a parameter. The 3-body problem we started with has been reduced to a set of 2-body problems, one for each value of $\boldsymbol{r}$. The resulting solution $\phi^{\mathrm{Adia}}(\boldsymbol{R}, \boldsymbol{r})$ is a superposition of all the projectile states $(\phi_i(\boldsymbol{r}), \phi_{\boldsymbol{k}}(\boldsymbol{r}))$.

The adiabatic approximation to the transition amplitude to a particular projectile state is calculated by projecting onto that state and examining the coefficient of the outgoing wave for R asymptotically large. If $f(\theta, \phi, \boldsymbol{r})$ is the scattering amplitude in the direction θ, ϕ calculated from eq.(98) for a fixed value of $\boldsymbol{r}$, then the scattering amplitude for exciting state i is

$$f_{i0} = \int d\boldsymbol{r}\phi_i^*(\boldsymbol{r})f(\theta, \phi, \boldsymbol{r})\phi_0(\boldsymbol{r}). \tag{99}$$

Examples of the application of this method to composite particle scattering including several frozen degrees of freedom can be found in refs. [19–23]. When the 2-body scattering problem eq.(98) is solved using the additional assumption of straight line trajectories in $\boldsymbol{R}$-space the results are equivalent to Glauber's [18] theory. Calculations along these lines [1,2,39,24,25,42] have been of great importance in the interpretation of reaction cross sections for halo nuclei in terms of nuclear sizes. Some of the earlier calculations used a further approximation to Glauber's many body theory theory known variously as the 'optical limit', the 'static limit', or the 'folding model'. It has been proved recently [27] that for a given halo wave function the 'folding model' always overestimates the total reaction cross section for strongly absorbed particles. Published complete Glauber calculations [24,25,42] are consistent with this theorem.

It is clearly desirable to convert the adiabatic condition eq.(97) into a quantitative estimate expressed in terms of the parameters of the collision process of interest and to devise methods of calculating the leading corrections to the adiabatic scattering amplitudes. It is clear that eq.(97) requires small projectile excitation energies (slow halo degrees of freedom) and high incident energies (short collision times). Qualitative estimates along these lines can be found in refs. [18,32,33], and some progress has been made in deriving correction terms for transfer reactions [28] and elastic scattering [34]. Here we shall assume that the adiabatic approximation is adequate and confine ourselves to the scattering of halo nuclei at energies for which a simple estimate indicates there is a good case for this to be a valid starting point.

The adiabatic approximation can also be regarded as an approximate solution of the coupled equations eq.(91) when all the channel energies E_i are assumed to be degenerate and equal to E_0. Multiplying the ith equation by $\phi_i(\boldsymbol{r})$, summing up all the equations over i using the completeness of the $\phi_i(\boldsymbol{r})$, one obtains an equation equivalent to eq.(98) with ϕ identified as $\sum \phi_i \chi_i$. This derivation does not give an immediate indication of the conditions for the validity of the approximation.

A recent review of many applications of the adiabatic approximation to few-body models of the scattering of halo nuclei can be found in [29].

4.2 Special cases

Implementation of the adiabatic approximation requires the calculation of scattering solutions $\phi^{\rm Adia}(\boldsymbol{R}, \boldsymbol{r})$ of eq.(98). Eq.(98) for fixed $\boldsymbol{r}$ is equivalent to a 2-body problem in a potential which is non-central, even if V_{nt} and V_{CT} are themselves central, and an exact solution requires the solution of coupled equations [19,20,23]. There are 2 cases when an enormous simplification occurs:

1. *When $\phi^{\rm Adia}(\boldsymbol{R}, \boldsymbol{r})$ is required at the point $r = 0$ only.*
   Eq.(98) then reduces to a 2-body central force problem in the potential $V_{nT}(R) + V_{CT}(R)$. This insight has been exploited [19,30,28] to give a theory of deuteron stripping and pick-up which includes deuteron break-up effects in a simple way.

2. *When one of the interactions, V_{nT} say, between the constituents of the projectile and the target is zero [31].*
   We shall refer to this special case as 'the recoil model' because the only way the projectile can be excited or broken up is through recoil of the core following scattering by the target. Note that the other 2 interactions V_{nC} and V_{CT} can be of arbitrary strength or range and may include Coulomb terms.

In case 2 the exact solution of eq.(98) corresponding to a projectile in its ground state ϕ_0 incident with momentum $\boldsymbol{K}$ on a target T is [31,33,32]

$$\phi_{\boldsymbol{K}}^{(+)\mathrm{A}dia}(\boldsymbol{r},\boldsymbol{R}) = \phi_0(\boldsymbol{r}\,)\, e^{i\alpha\boldsymbol{K}\cdot\boldsymbol{r}} \chi_{\boldsymbol{K}}^{(+)}(\boldsymbol{R}-\alpha\boldsymbol{r}), \tag{100}$$

where $\chi_{\boldsymbol{K}}^{(+)}$ is a distorted wave which describes the scattering of a particle of mass μ_{PT} (the projectile-target reduced mass) from the potential V_{CT}, *i.e.*,

$$\begin{aligned}[T_{R'} + V_{CT}(\boldsymbol{R}'))]\ \chi_{\boldsymbol{K}}^{(+)}(\boldsymbol{R}') &= E_K \chi_{\boldsymbol{K}}^{(+)}(\boldsymbol{R}'),\\ \chi_{\boldsymbol{K}}^{(+)}(\boldsymbol{R}') &\stackrel{R'\to\infty}{\to} \exp(i\boldsymbol{K}\cdot\boldsymbol{R}') + f_{CT}\exp(iKR')/R'\ .\end{aligned} \tag{101}$$

Note that in eq.(100) the distorted wave has the argument $(\boldsymbol{R}-\alpha\boldsymbol{r})$, which is just the $C-T$ separation. The distorted wave corresponds to a model in which all effects due to the halo neutron are ignored apart from its contribution to the mass of the projectile. In the following we will refer to this limit as the scattering of a 'no-halo' projectile.

We emphasise that the three-body wave function, eq.(100), includes components which describe break-up and excitations of the projectile. This is clear from the complicated dependence on $\boldsymbol{r}$, through the argument of $\chi_{\boldsymbol{K}}^{(+)}$ and the exponential factor $\exp(i\alpha\boldsymbol{K}\cdot\boldsymbol{r})$ which will result in a non-vanishing overlap with any of the states $(\phi_i(\boldsymbol{r}), \phi_{\boldsymbol{k}}(\boldsymbol{r}))$.

4.3 Applications of the adiabatic 'recoil model'

The exact elastic scattering transition amplitude for the projectile, from initial state $\boldsymbol{K}$ into final state $\boldsymbol{K'}$, is

$$T_{\mathrm{el}}(\boldsymbol{K}',\boldsymbol{K}) = \int d\boldsymbol{r} \int d\boldsymbol{R}\ \phi_0^*(\boldsymbol{r}\,)\ e^{-i\boldsymbol{K}'\cdot\boldsymbol{R}}\ V_{CT}(\boldsymbol{R}-\alpha\boldsymbol{r}\,)\ \Psi_{\boldsymbol{K}}^{(+)}(\boldsymbol{r},\boldsymbol{R}), \tag{102}$$

where $\Psi_{\boldsymbol{K}}^{(+)}(\boldsymbol{r},\boldsymbol{R})$ is the exact scattering state solution of eq.(8)

Using the adiabatic approximation to $\Psi_{\boldsymbol{K}}^{(+)}$, eq.(100), and making the change of variable from $\boldsymbol{R}$ to $\boldsymbol{R}' = \boldsymbol{R}-\alpha\boldsymbol{r}$ this factorises as

$$\begin{aligned}T_{\mathrm{el}}(\boldsymbol{K}',\boldsymbol{K}) = &\left[\int d\boldsymbol{r}\,|\phi_0(\boldsymbol{r}\,)|^2\ e^{i\alpha(\boldsymbol{K}-\boldsymbol{K}')\cdot\boldsymbol{r}}\right]\\ &\times\left[\int d\boldsymbol{R}'\ e^{-i\boldsymbol{K}'\cdot\boldsymbol{R}'}\ V_{CT}\ (\boldsymbol{R}')\ \chi_{\boldsymbol{K}}^{(+)}(\boldsymbol{R}')\right].\end{aligned} \tag{103}$$

The second integral here is just the transition amplitude $T_{\mathrm{no-halo}}(\boldsymbol{K}', \boldsymbol{K})$ for a 'no-halo' projectile scattering by the core-target potential V_{cT}. The same result for T_{el} is obtained by examining the asymptotic form of eq.(100) in the elastic channel.

The effects of projectile excitation and structure in eq.(103) arise entirely through the first integral, the form factor

$$F(\boldsymbol{Q}) = \int d\boldsymbol{r}\, |\phi_0(\boldsymbol{r}\,)|^2 \ \exp(i\boldsymbol{Q}\cdot\boldsymbol{r}), \tag{104}$$

where $\boldsymbol{Q} = \alpha(\boldsymbol{K} - \boldsymbol{K}')$.The corresponding elastic scattering differential cross section is therefore

$$\left(\frac{d\sigma}{d\Omega}\right)_{el} = |F(\boldsymbol{Q})|^2 \times \left(\frac{d\sigma}{d\Omega}\right)_{\mathrm{no-halo}}, \tag{105}$$

where $(d\sigma/d\Omega)_{\mathrm{no-halo}}$ is the cross section for a projectile, with mass μ, scattering by the core-target interaction and is therefore very closely related to the experimental core-target elastic scattering.

The importance of eq.(105) is that it clarifies the relevant scattering angles and incident energies at which a halo of a given size and structure will be manifest as a deviation from the scattering due to a projectile which does not have the spatial extension associated with a loosely bound halo particle.

Eq. (105) is reminiscent of factorisations which occur in electron scattering when Born approximation and approximate distorted wave theories are used. Note, however, that the present analysis does not involve Born approximation in any sense. Only if all intermediate states are included do the second and higher order terms in the Born series factorise in this way [33]. The same argument obtains for the factorisation of the wavefunction in eq.(100).

^{11}Be is a good example of a binary, ^{10}Be+n, single neutron halo nucleus and ^{19}C is also a single neutron halo candidate [35]. Both systems have small $\alpha = m_n/m_P$ ratios. For ^{11}Be+^{12}C, there are small angle elastic scattering data [36] for both the ^{10}Be core and the ^{11}Be composite, but at energies of 59.4 MeV/A and 49.3 MeV/A, respectively. Ideally these data are required at the same energy per nucleon to provide the necessary information on V_{CT}, which is an essential ingredient in applications of eq.(105).

According to eq.(105) the formfactor $|F(Q)|^2$, which multiplies the point particle cross section, reflects the modifications to the scattering due to the composite nature of the projectile. In Figure 2 we show calculated squared formfactors as a function of the centre-of-mass angles which are appropriate for the elastic scattering of ^{11}Be (upper part) and ^{19}C (lower part) from ^{12}C at 49.3 MeV/A and 30 MeV/A, respectively. These calculations demonstrate the sensitivity of the formfactor to the halo properties. Conversely, they demonstrate the information about the halo-core relative motion wavefunction which is available in principle from halo nucleus elastic scattering data.

The strong deviations from unity shown in Figure 2 reflect in momentum space the long exponential tails of the halo wavefunctions we discussed in Section

1.1. In the notation of that Section, a neutron wavefunction with a λ-value corresponding to a typical non-halo nucleus the formfactor would hardly deviate at all from unity over the angular range of Figure 2.

For ^{11}Be, the halo is seen to result in a reduction in the elastic differential cross section by a factor of between 2 and 4 at 20°, compared to that for 'no-halo' scattering. There is also a significant sensitivity to the assumed rms separation of the valence and core particles.

For ^{19}C, the squared formfactors which result from a pure $2s_{1/2}$ (solid curve) or $1d_{5/2}$ (dashed curve) neutron state are shown. The departures from 'no-halo'

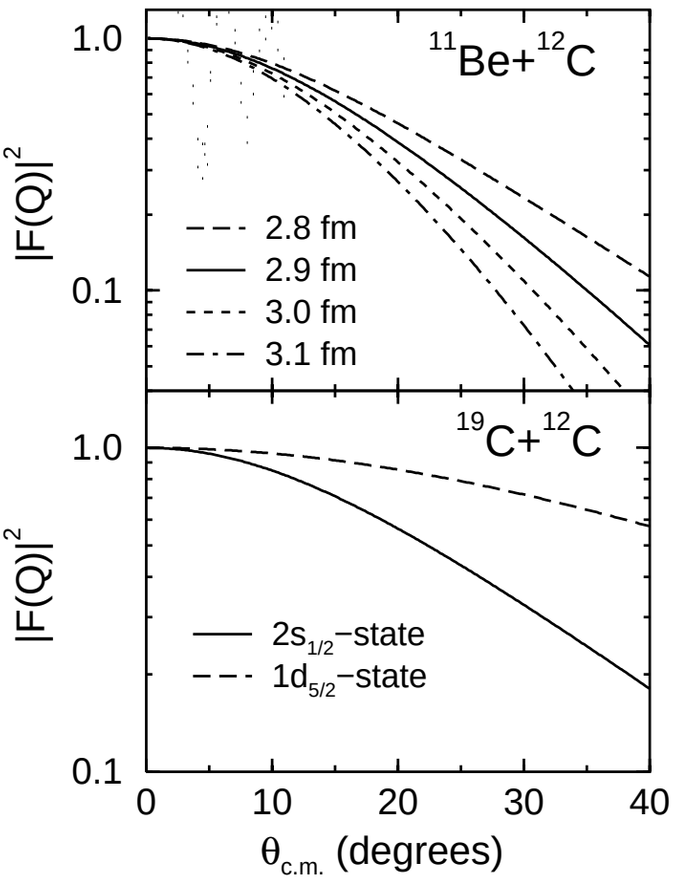

Fig. 2. Calculated $|F(Q)|^2$, as a function of centre-of-mass scattering angle for the elastic scattering of ^{11}Be (upper part) and ^{19}C (lower part) from ^{12}C at 49.3 MeV/A and 30 MeV/A, respectively.

scattering are predicted to be significantly different for a $2s_{1/2}$ and $1d_{5/2}$ valence neutron, with almost a factor of 2 difference in the cross sections at 20°. We note that, although the leading term in the expansion of the formfactor about $Q = 0$ gives a deviation from unity proportional to the mean squared separation of the core and valence particles in the projectile, the values of Q which enter in the examples above are such that this leading order term is inadequate and there is sensitivity to higher order moments except at the very smallest angles.

For ^{11}Be the wavefunctions were taken to be pure $2s_{1/2}$ neutron single particle states, with separation energy 0.503 MeV, calculated in a central Wood-Saxon potential [37]. By changing the binding potential geometry we generate ^{11}Be composites with different rms matter radii and hence $|F(Q)|^2$. For ^{19}C the ground state structure is presently uncertain with speculations of it being a pure $2s_{1/2}$ state, $1d_{5/2}$ state or a linear combination of such configurations [38]. The neutron separation energy was 0.240 MeV.

Figure 3 shows the elastic differential cross section angular distributions (ratio to Rutherford) for ^{11}Be+^{12}C scattering at 49.3 MeV/A calculated with a number of different models of the scattering mechanism.

The dashed curve shows the 'no-halo' projectile differential cross section $(d\sigma/d\Omega)_{\mathrm{no}-halo}$ calculated using the core-target potential. It might be expected that the main effect of the extended size of the projectile could be accounted for by calculating the scattering by a potential $V_{\mathrm{fold}}(R)$ which averages $V_{nT}(\boldsymbol{R}+\beta\boldsymbol{r})+V_{CT}(\boldsymbol{R}-\alpha\boldsymbol{r})$ over the probability density for $\boldsymbol{r}$ predicted by the ground state halo density, *i.e.*

$$V_{\mathrm{fold}}(R) = \int d\boldsymbol{r}[V_{nT}(\boldsymbol{R}+\beta\boldsymbol{r}) + V_{CT}(\boldsymbol{R}-\alpha\boldsymbol{r})]|\phi_0(r)|^2. \qquad (106)$$

The dot-dashed curve in Figure 3 shows the cross section calculated using the folding model interaction, eq.(106) . The similarity of the folding and 'no-halo' calculations makes clear that the effects associated simply with folding the core and valence particle interactions over the size of the halo are relatively minor compared with the effects taken into account in the solid curve. The latter is obtained using the result eq.(105) with the squared formfactor shown by the short dashed line (the 2.9 fm rms case of Fig.2).

The physical difference between the theory which produces the solid line and the 'folding' result is that the former does not assume that the projectile remains in its ground state during the scattering but correctly takes into account (insofar as the adiabatic approximation is adequate) the large projectile excitation and break up effects induced by the target. It is remarkable that such complicated multistep processes are fully accounted for by eq.(105) when the interaction between the halo and the target is ignored. Note, however, that at small angles the 'folding' diffraction pattern is shifted to smaller angles as one would expect for the more spatially extended potential of eq.(106).

We recall that the special case under discussion ignores the interaction between the valence neutron and the target. In fact this interaction is not negligible and must be taken into account in a detailed comparison with experiment. This

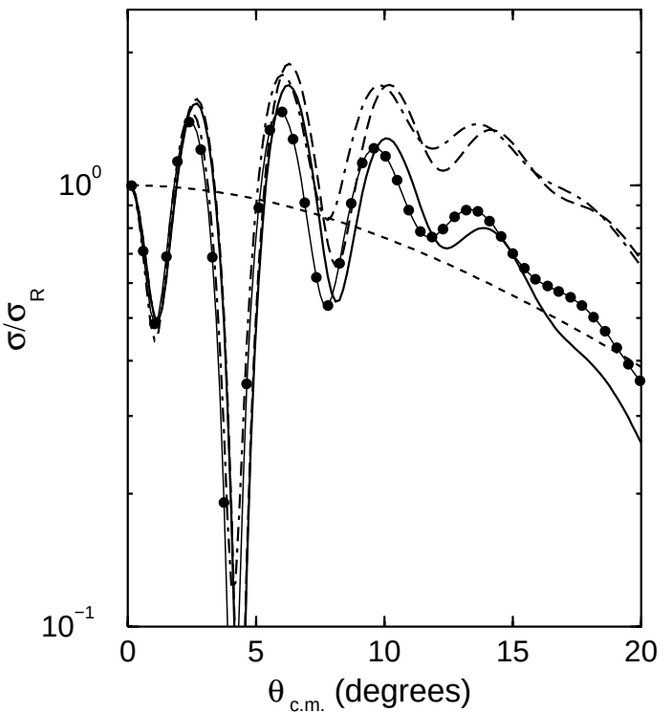

Fig. 3. Calculated elastic differential cross section angular distributions (ratio to Rutherford) for ^{11}Be+^{12}C scattering at 49.3 MeV/A. The curves are discussed in the text.

is not a difficulty since exact adiabatic calculations which include the interaction between all the halo particles and the target are possible for both two and three-body projectile systems [23,22]. Such calculations have also been carried out for 4- and 5-body projectiles within the eikonal approximation [40,41].

In Figure 4 we show the results of such adiabatic calculations for ^{11}Be+^{12}C scattering at 49.3 MeV/A. These include the neutron+^{12}C optical potential tabulated in [43], and correspond to the four ^{11}Be wavefunctions with different rms radii discussed in connection with Figure 2. The data are from [36]. We note that the behavior of the cross sections expected on the basis of the formfactors of Figure 2 and the insights the 'recoil model' provides are not effected in any major way by the neutron-target interaction. These results suggest that elastic scattering data of sufficient quality could yield independent information on halo structures.

The full circle symbols in Figure 3 are also full adiabatic model calculation including V_{nT}. They can be compared with the solid line results which are also adiabatic but do not include V_{nT}. The agreement is reasonable and suggests that

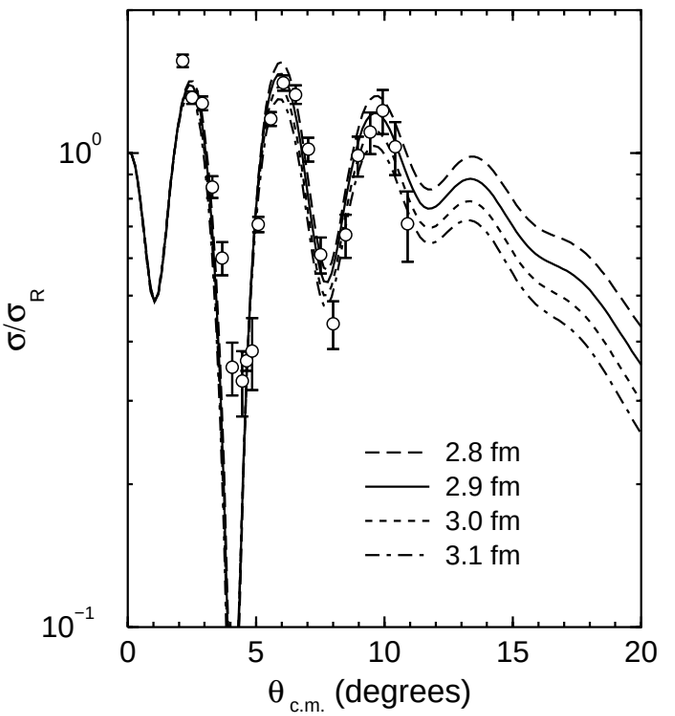

Fig. 4. Calculated elastic differential cross section angular distributions (ratio to Rutherford) for ^{11}Be+^{12}C scattering at 49.3 MeV/A calculated using the adiabatic approximation and including the neutron-target interaction.

V_{CT} dominates in this system, although the effects of the valence neutron-target interaction are not negligible.

The 'recoil model' teaches us that halo nucleus elastic scattering angular distributions are strongly affected by projectile excitation channels and the spatial size of the halo. These effects are principally manifest through a formfactor which depends only on the halo ground state wavefunction and whose square multiplies the 'no halo' cross section. The latter is defined to be the cross section for a particle with the mass of the projectile but which interacts with the target through the core-target potential with no folding in of the halo density. This potential is in principle to be obtained from core-target scattering at the same energy per nucleon as that of the halo nucleus scattering of interest. In fact to a good approximation at the energy used in Figure 2 the 'no halo' cross section can be evaluated directly from the core-target cross section at the same energy per nucleon and momentum transfer.

5 Other applications of the 'recoil model'

We have already mentioned the application of the adiabatic approximation to the calculation of reaction cross sections for halo nuclei in Sub-section 4.1. The approximation has also been widely used to treat deuteron break-up effects in stripping and pick-up reactions (see [28] and [48] and references therein). The special case of the 'recoil model' has had some other interesting recent applications.

5.1 Coulomb break-up of neutron halo nuclei

One situation when the neglect of the interaction between the halo neutron and the target can be justified is when Coulomb forces dominate. We will now explain how the 'recoil model' can be used used as the starting point of a non-perturbative quantum mechanical theory of the Coulomb break-up of neutron halo nuclei. [45–47].

Some care is required in using the adiabatic wavefunction to calculate break-up amplitudes. The explicit form of the solution eq.(100) makes it clear that at large core-neutron separations, $r \to \infty$, the presence of the factor ϕ_0 means that, independently of the details of the 3-body Hamiltonian, $\phi_{\boldsymbol{K}}^{(+)\mathrm{A}dia}(\boldsymbol{r}, \boldsymbol{R})$ vanishes exponentially. The large r region is where one would expect to look for breakup flux and therefore $\phi_{\boldsymbol{K}}^{(+)\mathrm{A}dia}(\boldsymbol{r}, \boldsymbol{R})$ can not be used to calculate break-up amplitudes by looking at its asymptotic form.

It follows that to use the three-body wave function of eq.(100) to calculate a Coulomb breakup amplitude we must restrict its use to regions of the six-dimensional ($\boldsymbol{r}$,$\boldsymbol{R}$) space where r is finite. In particular, we do not attempt to extract the breakup amplitude from the asymptotics of our approximate adiabatic solution. Ref [45] procceeds instead as follows.

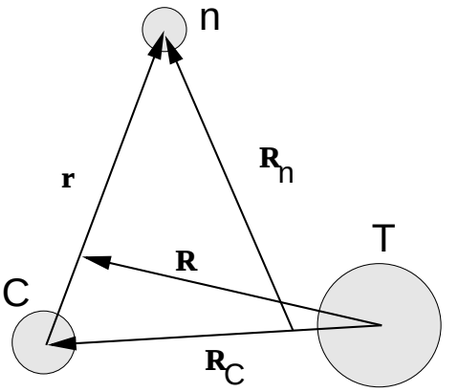

Fig. 5. Definition of the co-ordinate system adopted for the core, valence, and target three-body system.

We first rewrite the *exact* three-body Schrödinger equation of eq. (8), prior to having made any adiabatic approximation, as

$$[E - T_{\boldsymbol{R}_n} - T_{\boldsymbol{R}_C} - V_{CT}(\boldsymbol{R}_C)]\,\Psi^{(+)}_{\boldsymbol{K}}(\boldsymbol{r},\boldsymbol{R}) = V_{nC}(\boldsymbol{r})\Psi^{(+)}_{\boldsymbol{K}}(\boldsymbol{r},\boldsymbol{R}) \quad . \tag{107}$$

where $T_{\boldsymbol{R}_n}$ and $T_{\boldsymbol{R}_C}$ are the kinetic energies in the coordinates $\boldsymbol{R}_n$ and $\boldsymbol{R}_C$. These Jacobi co-ordinates are defined so that $\boldsymbol{R}_n$ connects n with the centre-of-mass of C and T, and $\boldsymbol{R}_C$ is the $C-T$ separation (see Figure 5). They are particularly suitable when $V_{nT} = 0$.

Because of the short ranged factor $V_{nC}(\boldsymbol{r})$ the right-hand-side eq.(107) requires the wqavefunction $\Psi^{(+)}_{\boldsymbol{K}}(\boldsymbol{r},\boldsymbol{R})$ only for finite separations $\boldsymbol{r}$. We can therefore justifiably evaluate it using the adiabatic wavefunction $\phi^{(+)\mathrm{A}dia}_{\boldsymbol{K}}(\boldsymbol{r},\boldsymbol{R})$ as a good approximation to $\Psi^{(+)}_{\boldsymbol{K}}$. This yields the inhomogeneous equation

$$[E - T_{\boldsymbol{R}_n} - T_{\boldsymbol{R}_C} - V_{CT}(\boldsymbol{R}_C)]\,\hat{\Psi}^{(+)}_{\boldsymbol{K}}(\boldsymbol{r},\boldsymbol{R}) = V_{nC}(\boldsymbol{r})\phi^{(+)\mathrm{A}dia}_{\boldsymbol{K}}(\boldsymbol{r},\boldsymbol{R}) \tag{108}$$

For a given adiabatic wavefunction eq.(108) can be solved using Green function techniques to give a solution which has the correct 3-body asymptotics [45] and from which an expression for the break-up amplitude into any final state can be read off. The break-up amplitude calculated in this way for a three-body final state with Jacobi momenta $\boldsymbol{q}_C$ and $\boldsymbol{q}_n$ corresponding to $\boldsymbol{R}_n$ and $\boldsymbol{R}_C$, is found to be [45]

$$\bar{T}_{\mathrm{A}D}(\boldsymbol{q}_n\boldsymbol{q}_C,\boldsymbol{K}) = \left\langle e^{i\boldsymbol{q}_n\cdot\boldsymbol{R}_n}\chi^{(-)}_{\boldsymbol{q}_C}(\boldsymbol{R}_C)\,|V_{nC}(\boldsymbol{r})|\,\bar{\Psi}^{(+)}_{\boldsymbol{K}}(\boldsymbol{r},\boldsymbol{R})\right\rangle \ , \tag{109}$$

where $\chi^{(-)}_{\boldsymbol{q}_C}$ is an Coulomb distorted wave with in-going scattered waves describing the scattering of the outgoing core by the target.

It is shown in [45] that the break-up amplitude $\bar{T}_{\mathrm{A}D}$ of eq.(109) is exactly the same as the expression obtained by using the adiabatic wavefunction directly in the exact post-form transition amplitude.

Note that although the adiabatic approximation neglects the projectile excitation energy in the calculation of the adiabatic three-body wavefunction $\bar{\Psi}^{(+)}_{\boldsymbol{K}}$, this does not mean that the break-up amplitude is calculated using the the zero adiabaticity parameter $\xi = 0$ limit, of semi-classical theories [49]. As the analysis above shows, $\bar{T}_{\mathrm{A}D}$ includes a final state wavefunction with the correct kinematics and excitation energies required by energy conservation, unlike analogous $\xi = 0$ semi-classical calculations.

5.2 Break-up transition amplitude

It is shown in [45] that the amplitude $\bar{T}_{\mathrm{A}D}$ of eq.(109) factorises exactly as

$$\begin{aligned}
\bar{T}_{\mathrm{A}D}(\boldsymbol{q}_n\boldsymbol{q}_C,\boldsymbol{K}) \quad &= \quad \left[\int d\boldsymbol{r}\, e^{-i\boldsymbol{P}_n\cdot\boldsymbol{r}}V_{nC}(\boldsymbol{r})\phi_0(\boldsymbol{r})\right] \\
&\quad \times \left[\int d\boldsymbol{R}_C\, e^{-i\boldsymbol{Q}_n\cdot\boldsymbol{R}_C}\chi^{(-)*}_{\boldsymbol{q}_C}(\boldsymbol{R}_C)\chi^{(+)}_{\boldsymbol{K}}(\boldsymbol{R}_C)\right] \\
&= \quad \langle \boldsymbol{P}_n|V_{nC}|\phi_0\rangle \ \left\langle \boldsymbol{Q}_n,\chi^{(-)}_{\boldsymbol{q}_C}|\chi^{(+)}_{\boldsymbol{K}}\right\rangle \quad ,
\end{aligned} \tag{110}$$

where we have defined $\boldsymbol{P}_n = \boldsymbol{q}_n - \alpha\boldsymbol{K}$ and $\boldsymbol{Q}_n = \frac{m_T}{m_T+m_C}\boldsymbol{q}_n$.

The two factors in Eq.(110) separate out the structure and dynamical parts of the calculation. The overlap of the three continuum functions, $\langle \boldsymbol{Q}_n, \chi^{(-)}_{\boldsymbol{q}_C} | \chi^{(+)}_{\boldsymbol{K}} \rangle$, can be evaluated in closed form and expressed in terms of the bremsstrahlung integral [45]. This factor now contains all the dynamics of the breakup process and is readily calculated for given incident and outgoing momenta in terms of the charges and masses of C and T.

The structure of the projectile enters through the vertex function $\langle \boldsymbol{P}_n | V_{nC} | \phi_0 \rangle$ and is also simply evaluated given any structure model for the projectile. In Coulomb dissociation, momentum can be transferred to the valence particle only by virtue of its interaction V_{nC} with the core. Since the term $\alpha \boldsymbol{K}$ in $\boldsymbol{P}_n$ is the fraction of the incident momentum of the projectile which is carried by the valence particle, this structure vertex displays explicitly this momentum transfer from the ground state via V_{nC}.

The result (110) allows a fully finite-range treatment of the core-neutron particle interaction V_{nC} without any approximation additional to the adiabatic assumption. The theory is thus applicable to projectiles with any ground state orbital angular momentum structure, and also includes breakup contributions from all contributing Coulomb multipoles and relative orbital angular momenta between the neutron and core fragments. Unlike DWBA theories it includes the initial and final state interactions V_{CT} and V_{nC} to all orders.

The theory has been successfully applied to the break-up of high energy deuterons in the forward direction [45,50], and with appropriate generalisation, to the Coulomb break-up of one- and two-neutron halo nuclei [46,47]. Here we briefly mention the case of deuteron break-up.

The (d, pn) elastic breakup data have been measured at the RIKEN Accelerator Research Facility, Saitama, at 140 and 270 MeV, and at the Research Centre for Nuclear Physics (RCNP), Osaka, at 56 MeV in a kinematical condition of $\theta_p \approx \theta_n \approx 0^\circ$. The targets were ^{12}C, ^{28}Si, ^{40}Ca, ^{90}Zr, ^{118}Sn, ^{165}Ho and ^{208}Pb at E_d=140 and 270 MeV and ^{12}C, ^{40}Ca, ^{90}Zr, and ^{208}Pb at E_d=56 MeV.

The calculations and data at 140 MeV are compared in Figure 6 for all measured targets. The errors shown in the figure are statistical only. The solid lines show the elastic breakup cross sections, as a function of the detected (laboratory) proton energy, calculated using eq.(110). The overall agreement of the calculated magnitudes, Z_T-dependence, and the proton energy dependence, with the data is good and improves with increasing target charge. The factor of 40 increase in the magnitudes of the measured cross sections in going from ^{12}C to ^{208}Pb is seen to be well reproduced as a function of Z_T. Figure 6 does not, however, reveal the complex way that the calculated cross sections are built up in the integrations over the experimental solid angle acceptances. We refer to refs. [45,50] for these crucial considerations and for a full discussion of the results at all 3 incident energies.

We emphasise again that these calculations are non-perturbative and fully quantum mechanical. They are based on a theory which is very different from the DWBA both in principle and in terms of the numerical results obtained.

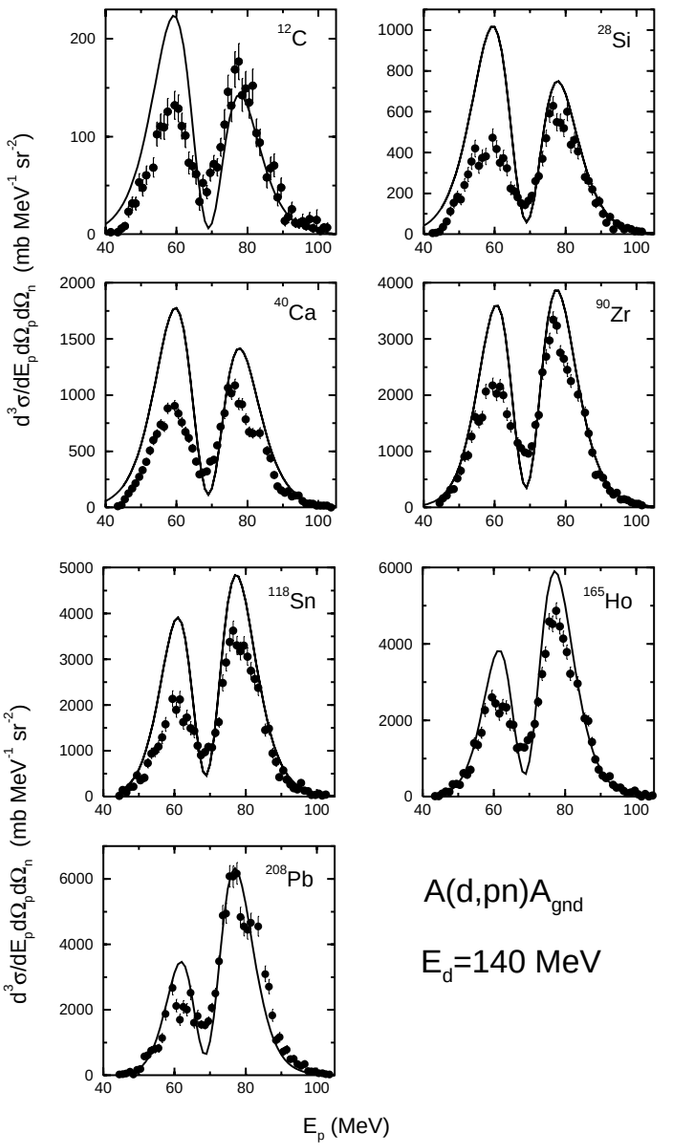

Fig. 6. Experimental and calculated adiabatic model (solid curves) triple differential cross sections for deuteron break-up near 0° in the laboratory frame at E_d =140 MeV. The calculations are averaged over the neutron and proton solid angles actually used in the experiment. The data are from ref.[50].

These differences are discussed in detail in ref. [45]. Final state interactions between the outgoing fragments are fully taken into account, apart from the nuclear interaction between the neutron and the target. The nuclear interaction between the neutron and the proton is accounted for to all orders.

The results of ref.[45,50] are consistent with an underlying physical picture in which Coulomb breakup is the dominant mechanism. There are, however, indications of a missing and interfering contribution, particularly on the lighter targets which may result from breakup by the nuclear forces between the projectile and the target which are ignored in the model of refs. [45,50].

5.3 Deuteron stripping and pick-up on halo nuclei

We have already mentioned the use of the adiabatic approximation to treat multi-step processes via deuteron break-up channels in stripping and pick-up reactions. This is special case 1. of Sub-section 4.2. A recent development has been to use the adiabatic approximation to additionally treat excitations of a halo nucleus produced as the final state in a (d,p) reaction. It is shown in ref. [48] how the simplicity of the 'recoil model' can be exploited to give a very convenient way of evaluating what would otherwise be a very complicated multi-channel calculation. See also [34] for an application to recent ^{11}Be(p,d)^{10}Be data from GANIL [51].

6 Conclusions

I hope I have conveyed to you some of the fascination of nuclear reactions with halo and other weakly bound nuclei. New experiments are giving a new challenge to theory. Groups in Surrey and elsewhere are working very hard to meet this challenge.

A particular challenge to theory is to understand and evaluate the leading corrections to the adiabatic theory and to learn how to apply them to transfer and break-up reactions. There is also a need to understand how the few-body models of reactions described here can be related to the underlying many-fermion structure of the halo nucleus.

Acknowledgements

I am grateful to J.M. Arias and M. Lozano for giving me the opportunity to come to Seville and lecture at their Summer School. I very much enjoyed meeting and discussing physics with the participants.

References

1. I. Tanihata H. Hamagaki, O. Hashimoto, S. Nagamiya, Y. Shida,N. Yoshikawa, O. Yamakawa, K. Sugimoto, T. Kobayashi, D.E. Greiner, N. Takahashi, and Y. Nojiri, Phys. Lett. **B160**, 380 (1985)

2. I. Tanihata, T. Kobayashi, O. Yamakawa, T. Shimoura, K. Ekuni, K. Sugimoto, N. Takahashi, T. Shimoda and H. Sato: Phys. Lett. **B206**, 592 (1988)
3. I. Tanihata, H. Hamagaki, O. Hashimoto, Y. Shida, N. Yoshikawa, K. Sugimoto, O. Yamakawa, T. Kobayashi, and N. Takahashi: Phys. Rev. Lett. **55**, 2676 (1985)
4. P.G. Hansen, A.S. Jensen and B. Jonson: Annual Rev. Nucl. Part. Sci. **45**, 591 (1995)
5. I.J. Thompson, B.V. Danielin, V.D. Efros, J.S. Vaagen, J.M. Bang, and M.V. Zhukov: Phys. Rev. **C61**, 024318 (2000)
6. H. Feshbach: Ann. Phys.(N.Y.) **5**, 357 (1958)
7. G. R. Satchler: "Direct Nuclear Reactions", Oxford University Press, Oxford, 1983
8. B. Lippmann and J. Schwinger: Phys. Rev. **79**, 469 (1950)
9. M.L. Goldberger and K M. Watson: "Collision Theory",Wiley, New York, 1964
10. R. Taylor: "Scattering Theory", Wiley, New York, 1972
11. D. M. Brink and G. R. Satchler: "Angular Momentum", 2nd Edition, Clarendon Press, Oxford, 1968
12. I.J. Thompson: Comp. Phys. Rep. **7**, 167 (1988)
13. I.J. Thompson: "Methods of direct reaction theory" in "Scattering" eds. R.Pike and P.Sabatier, Academic Press, Chapter 3.1.2, in the press
14. J. Gomez-Camacho and R.C. Johnson: "Polarisation in nuclear physics" in "Scattering" eds. R.Pike and P.Sabatier, Academic Press, Chapter 3.1.4, in the press
15. M. Kamimura, M. Yahiro, Y. Iseri, H. Kameyama, Y. Sakuragi and M. Kawai: Prog. Theor. Phys. Suppl. **89**, 1 (1986)
16. N. Austern, Y. Iseri, M. Kamimura, M. Kawai, G. Rawitscher and M. Yahiro: Phys. Rep. **154**, 125 (1987)
17. F.M. Nunes and I.J. Thompson: Phys. Rev. **C59**, 2652 (1999)
18. R. J. Glauber: in "Lectures in Theoretical Physics", edited by W E Brittin (Interscience, New York, 1959), Vol. 1, pp 315-414
19. R.C. Johnson and P.J.R. Soper: Phys. Rev. **C1**, 976 (1970)
20. H. Amakawa, S. Yamaji, A. Mori and K. Yazaki: Phys. Lett. **B82**, 13 (1979)
21. J.S. Al-Khalili and R.C. Johnson: Nucl. Phys. **A546**, 622 (1992)
22. J.A. Christley, J.S. Al-Khalili, J.A. Tostevin and R.C. Johnson: Nucl. Phys. **A624**, 275 (1997)
23. I.J. Thompson: Computer Programme ADIA, Daresbury Laboratory Report, 1984, unpublished
24. J.S. Al-Khalili and J.A. Tostevin: Phys. Rev. Lett. **76**, 3903 (1996)
25. J.S. Al-Khalili, I.J. Thompson and J.A. Tostevin: Phys. Rev. **C54**, 1843 (1996)
26. J.A. Tostevin, R.C. Johnson, J.S. Al-Khalili: Nucl. Phys. **A630**, 340c (1998)
27. R.C. Johnson and C.J. Goebel: Phys. Rev. **C61**, 027603 (2000)
28. A. Laid , J.A. Tostevin and R.C. Johnson: Phys. Rev. **C48**, 1307 (1993)
29. J.S. Al-Khalili and J.A. Tostevin: "Few-body models of nuclear reactions" in "Scattering" eds. R.Pike and P.Sabatier, Academic Press, Chapter 3.1.3, in the press
30. J. D. Harvey, R.C. Johnson: Phys. Rev. **C3**, 636 (1971)
31. R.C. Johnson, J.S. Al-Khalili, J.A. Tostevin: Phys. Rev. Lett. **79**, 2771 (1997)
32. R.C. Johnson: J. Phys. G: Nucl. Part. Phys. **24**, 1583 (1998)
33. R.C. Johnson: "Elastic scattering and elastic break-up of halo nuclei in a "recoil model" in Proc. Eur. Conf. On Advances in Nuclear Physics and Related Areas, Thessoloniki, Greece, July 8-12, 1997, (eds. D.M. Brink, M.E. Grypeos and S.E. Massen, Giahoudi-Giapouli, Thessaloniki, 1999) 156-162

34. R.C. Johnson, J.S. Al-Khalili, N.K.Timofeyuk and N. Summers: Nuclear reactions involving weakly bound nuclei, "Experimental Nuclear Physics in Europe", 21-26 June 1999, Seville, Spain (eds. B. Rubio, M. Lozano and W. Gelletly, AIP Conf Proc. 495 American Institute of Physics, 1999) 297-300
35. D. Bazin et al.: Phys. Rev. Lett. **74**, 3569 (1995)
36. P. Roussel-Chomaz: private communication, 1996
37. J.S. Al-Khalili, J.A. Tostevin and J.M. Brooke: Phys. Rev. **C55**, R1018 (1997)
38. D. Ridikas, M.H. Smedberg, J.S. Vaagen and M.V. Zhukov: Europhys. Lett. **37**, 385 (1997)
39. G.D. Alkhazov, M.N. Andronenko, A.V. Dobrovosky, P. Egelhof, G.E. Gavrilov, H. Geissel, H. Irnich, A.V. Khanzadeev, G.A. Korolev, A.A. Lobodenko, G. Münzenberg, M. Mutterer, S.R. Neumaier, F. Niskel, W. Schwab, D.M. Seliverstov, T. Suzuki, J.P. Theobald, N.A. Timofeev, A.A. Vorobyov and V.I. Yatsoura: Phys. Rev. Lett. **78**, 2313 (1997)
40. J.A. Tostevin, J.S. Al-Khalili, M. Zahar, M. Belbot, J. J. Kolata, K. Lamkin, D.J. Morrissey, B.M. Sherrill, M. Lewitowicz, A.H. Wuosmaa: Phys. Rev. **C56** R2929 (1997)
41. J.S. Al-Khalili and J.A. Tostevin: Phys. Rev **C57**, 1846 (1998)
42. J.A. Tostevin and J.S. Al-Khalili: Phys. Rev. **C59**, R5 (1999)
43. J.S. Al-Khalili, I.J. Thompson and J.A. Tostevin: Nucl. Phys. **A581**, 331 (1995)
44. J. A. Tostevin, R.C. Johnson and J.S Al-Khalili: Nucl. Phys. **A630**, 340c (1998)
45. J.A. Tostevin, S. Rugmai and R. C. Johnson: Phys. Rev. **C57**, 3225 (1998)
46. P. Banerjee, I. J. Thompson, and J. A. Tostevin: Phys. Rev. **C58** 1042 (1998)
47. P. Banerjee, J. A. Tostevin, and I. J. Thompson: Phys. Rev. **C58**, 1337 (1998)
48. N.K. Timofeyuk and R.C. Johnson: Phys. Rev. **C59**, 1545 (1999)
49. G. Baur, and H. Rebel: J. Phys. G: Nucl. Part. Phys. **20**, 1 (1994)
50. J.A. Tostevin, S. Rugmai, R.C. Johnson, H. Okamura , S. Ishida , N. Sakamoto, H. Otsu, T. Uesaka, T. Wakasa , H. Sakai , T. Niizeki, H. Toyokawa, Y. Tajima , H.Ohnuma, M. Yosoi, K. Hatanaka , T. Ichihara: Phys. Lett. **B424**, 219 (1998)
51. S. Fortier, S. Pita, J.S. Winfield, W.N. Catford, N.A. Orr, J. Van de Wiele, Y. Blumenfield, R. Chapman, S.P.G. Chappell, N.M. Clarke,N. Curtis, M. Freer, S. Gales, K.L. Jones, H. Langevin-Joliot, H. Laurent, I.Lhenry, J.M. Maison, P. Roussel-Chomaz, M. Shawcross, M. Smith, K. Spohr, T. Suomijarvi and A. de Vismes: Phys. Lett. **B461**, 2 (1999)